American Mineralogist, Volume 89, pages 564–571, 2004

The effect of TiO_2 on Pd, Ni, and Fe solubilities in silicate melts

ALEXANDER BORISOV,[1,3,*] YANN LAHAYE,[2] AND HERBERT PALME[3]

[1]Institute of Geology of Ore Deposits, Petrography, Mineralogy and Geochemistry Russian Academy of Sciences, Staromonetny 35, 109017 Moscow, Russia
[2]J.W. Goethe-Universität, Institut für Mineralogie (Abt. Petrologie und Geochemie), Senckenberganlage 28, 60054 Frankfurt, Germany
[3]Universität zu Köln, Institut für Mineralogie und Geochemie, Zülpicher Strasse 49b, 50674 Köln, Germany

ABSTRACT

We have determined Pd, Ni, and Fe solubilities in silicate melts of anorthite-diopside eutectic composition with variable TiO_2 concentrations, from TiO_2-free melts to melts with up to 26 wt% TiO_2. The experiments were conducted with metal loops at 1300 °C, one atm total pressure, and at a wide range of oxygen fugacities. The glasses were analyzed with the electron microprobe and by laser ablation inductively coupled plasma mass spectrometry (LA ICP-MS).

The behavior of Ni was found to be nonlinear. At given T-f_{O_2} conditions, its solubility is relatively constant for melts with up to about 4 wt% (3 mol%) TiO_2. At higher TiO_2 concentrations, Ni solubility increases strongly with TiO_2 contents. The results obtained for Pd at oxidizing conditions are similar to those obtained for Ni. The solubility of Fe increases uniformly with TiO_2 contents within the whole TiO_2 concentration range.

In some experiments Pd-containing alloy micronuggets were encountered. In this case analyses were done in areas free of nuggets. Experiments in which the nugget density was too high were discarded. The regular behavior of Pd—even in nugget-containing silicates—indicates that Pd-oxide solubility and nugget formation are independent processes.

The occurrence of Ti-rich phases (karrooite and armalcolite) on the liquidus of TiO_2-saturated melts at reducing conditions, and the Pd partition coefficients between rutile and silicate melts, were determined and are briefly discussed.

INTRODUCTION

The solubilities of noble metals (NM) in silicate melts of diopside-anorthite eutectic composition (DA) are well known from experimental work at one atm total pressure (Borisov et al. 1994; Borisov and Palme 1995, 1996, 1997; Borisov and Nachtweyh 1998; Ertel et al. 1999; Borisov and Walker 2000; Fortenfant et al. 2003). This melt composition may be considered as an Fe-free analogue of basaltic liquids and has been frequently used in experimental petrology when determining metal solubilities (Ni, Co, Mo, W, etc., see Holzheid et al. 1994; Ertel et al. 1996; O'Neill and Eggins 2002).

Possible effects of melt composition on NM solubilities are minor and may be ignored in calculating metal/silicate partition coefficients from solubilities, considering the very high metal/silicate partition coefficients of these elements (Borisov et al. 1994; Borisov and Palme 1995).

Because noble metals are fractionated during magmatic processes, they may be used as petrogenetic indicators (Barnes et al. 1988). However, quantification is difficult, as very little is known about the behavior of NM during rock-forming processes. In particular, it is still unclear which phases control the abundances of NM in a rock, either oxide minerals, sulfides, or native NM alloys. Borisov and Palme (2000) showed, for example, that primary mantle melts should be slightly oversaturated with Ir, Ru, and Pt, resulting in the formation of stable IrRuOs and PtFe alloys. For this kind of calculation, it is essential to know the solubilities of NM in silicate melts and the dependence of the solubilities on melt composition. Experimental studies of NM solubilities are, however, rare because of the so-called "nugget problem." This uncontrolled formation of metallic micro-inclusions in experimentally produced glasses often leads to incorrect results on noble metal solubilities, in particular with regard to the dependence of solubilities on pressure and S content (see discussions in Borisov and Palme 2000; Borisov and Walker 2000). Palladium seems to be a more-suitable element for these studies as nuggets were not encountered in the early work (Borisov et al. 1994).

Borisov et al. (1994) have analyzed silicate glasses using instrumental neutron activation analysis (INAA), which requires mechanical separation of the glass from the metals prior to analysis. New analytical techniques such as LA ICP-MS require very little sample preparation and are relatively fast and cost-effective. This technique also provides higher spatial resolution and allows NM dissolved as oxides and those present in metal nuggets to be distinguished (e.g., Ertel et al. 1999).

It is the main purpose of this paper to study the behavior of Pd in silicate melts in more detail. As first additive to the base DA composition TiO_2 was chosen. The addition of titania is known to affect physical properties of silicate melts (Dingwell 1992a, 1992b), Fe^{3+}/Fe^{2+} ratio (Gwinn and Hess 1989), or Fe solubility in silicate melts (Doyle 1989). Additionally, Xirouchakis et al. (2001) reported that the SiO_2 activity coefficients in silicate melts decrease with increasing TiO_2. Thus, one may expect a

* E-mail: aborisov@igem.ru

significant effect of the TiO_2 content on Pd solubility. Although terrestrial basalts almost never have more than 5 wt% TiO_2 due to saturation of magnetite or ilmenite (Toplis and Carroll 1995), we follow the common experimental practice of using a wide range of TiO_2 concentrations, from zero to rutile saturation, to better define possible effects.

Additional experiments involving Ni and Fe with the same spectrum of melt composition were performed to compare the behavior of NM and Fe-group metals.

Experimental procedures

The experiments were conducted with the loop technique in a 1-atm vertical tube furnace under controlled oxygen fugacity (uncertainties of cited $\log f_{O_2}$ values and temperature do not exceed ±0.1 and ±2 °C, respectively). Experimental conditions are listed in Tables 1 and 2.

The bands for loops were cut from Pd foil (0.1 mm thick and 99.95% pure, Chempure), Ni foil (0.125 mm thick, 99.9+% purity, Chempure), or Fe foil (0.2 mm thick, 99.7% purity, Chempure). The diameter of the loops was about 2.5 mm.

A synthetic Fe-free melt of anorthite-diopside eutectic composition (DA) was chosen as a base for the experiments. Appropriate amounts of TiO_2 were added to this composition to obtain mixtures with about 3% (DAT3), 5% (DAT5), 10% (DAT10), 17% (DAT17), and 32 wt% (DAT32) of TiO_2. The last composition is rutile-saturated at the experimental temperature of 1300 °C.

Up to six samples with different TiO_2 contents were simultaneously put into the furnace at given f_{O_2} conditions for 1–3 days. As demonstrated in earlier studies (Borisov 2001; O'Neill and Eggins 2002), a few hours at high temperatures are sufficient to equilibrate a melt with a metallic loop. After experiments, the samples were quenched by quickly withdrawing the sample holder from the hot zone to the top of the furnace. The samples were then mounted in epoxy and polished.

Bulk compositions of experimental glasses and crystalline phases, as well as Ni or Fe contents in silicate glasses were determined by electron probe microanalysis (EPMA) using a JEOL Superprobe (Universität zu Köln, Institut für Mineralogie und Geochemie). Natural corundum, diopside and rutile, and metallic Ni and Fe were used as standards. Operating conditions were 20 kV accelerating voltage, a beam current of 15 nA, and 20 s counting times. We used ZAF as a correction method. At least seven points were analyzed in each glass sample and the data were averaged.

Laser ablation ICP-MS analyses of experimental glasses were performed at the

Table 1. Experimental conditions, glass composition (wt%) and Pd solubility (ppm) in silicate melts of Di-An eutectic composition with variable TiO_2 contents

No.	Sample	$-\log f_{O_2}$	T °C	hs†	SiO_2	TiO_2	Al_2O_3	MgO	CaO	Total	Pd_ICP	s.d.	Pd_EMP	s.d.
1	DA-20	0.68*	1301	66	50.73	0.00	15.80	10.59	23.72	100.84	251	18	214	2
2	DAT3-20	"	"	"	49.74	2.23	15.30	10.32	23.24	100.83	262	3	219	5
3	DAT5-20	"	"	"	48.59	4.35	14.79	10.08	22.44	100.25	255	26	244	6
4	DAT10-20	"	"	"	45.90	8.55	14.10	9.59	21.07	99.22	370	5	302	7
5	DAT17-20	"	"	"	42.34	15.99	12.79	8.74	19.19	99.05	466	44	425	9
6	DAT32-20	"	"	"	38.02	24.99	11.29	7.64	17.07	99.00	609	35	609	14
7	DA-21	3.00	1301	64	50.27	0.00	16.06	10.86	23.78	100.97	41.5	1.1	-	-
8	DAT3-21	"	"	"	49.20	2.27	15.53	10.59	23.38	100.97	42.7	0.8	-	-
9	DAT5-21	"	"	"	49.13	4.15	15.09	10.12	22.48	100.98	39.9	3.2	-	-
10	DAT10-21	"	"	"	46.25	8.62	14.31	9.74	21.09	100.02	53.2	1.3	-	-
11	DAT17-21	"	"	"	42.08	16.27	12.98	8.90	19.20	99.42	75.0	3.2	-	-
12	DAT32-21	"	"	"	37.86	25.06	11.52	7.86	17.18	99.48	110.7	1.0	-	-
13	DAT17-6	9.84	1300	64	41.62	17.17	12.52	8.72	18.99	99.02	2.30	0.27	-	-
14	DAT32-6	"	"	"	37.01	26.29	10.95	7.82	17.12	99.18	2.57	0.17	-	-
15	DAT10-7	10.44	1300	65	45.63	9.33	13.91	9.61	20.88	99.36	1.24	0.11	-	-
16	DAT32-7	"	"	"	37.49	26.54	10.98	7.81	17.09	99.92	2.10	0.14	-	-
17	DAT10-4	10.61	1300	50	44.97	9.89	13.81	9.57	20.77	99.01	1.03	0.02	-	-
18	DAT17-4	"	"	"	41.53	16.99	12.74	8.76	18.99	99.01	1.34	0.01	-	-
19	DAT17-1	10.91	1301	46	41.68	16.77	12.70	8.75	19.12	99.01	1.06	0.02	-	-
20	DAT32-17	10.75	1300	68	36.87	26.69	10.93	7.58	16.98	99.05	1.86	0.03	-	-
21	DAT32-11	10.99	1301	67	36.70	27.46	10.66	7.72	17.35	99.88	1.82	0.06	-	-
22	DAT32-5	11.26*	1298	65	37.05	26.99	10.95	7.77	17.33	100.09	1.41	0.05	-	-
23	DAT32-5a	"	"	"	38.22	26.35	11.02	7.20	17.68	100.47	1.48	0.05	-	-
24	DAT32-12	11.47	1300	67	37.85	26.57	10.90	6.78	17.99	100.10	1.55	0.08	-	-

Notes: " = no changes in experimental conditions (the same run); s.d. = standard deviation; Pd_ICP = LA ICP-MS measurments; Pd_EMP = electrone micoprobe measurments using DAT32-20 with 609 ppm Pd as standard; all DAT32-ii melts are rutile saturated, DAT32-5a contains additionally karrooite, DAT32-12 contains only karrooite (see text for details).
* Calculated f_{O_2} (in all other runs a solid electrolyt sensor was used).
† Duration of experiment in hours.

Table 2. Glass composition (wt%) and calculated NiO and FeO activity coefficients in silicate melts of Di-An eutectic composition with variable TiO_2 contents

No.	SiO_2	TiO_2	Al_2O_3	MgO	CaO	MeO (s.d.)	Total	X_{TiO2}	X_{MeO}	γ_{MeO}
					Ni-loop experiments*					
1	50.04	0.00	15.57	10.45	23.27	1.62 (0.03)	100.98	0.0000	0.0129	3.16
2	48.48	2.23	15.23	10.47	22.93	1.65 (0.04)	100.99	0.0167	0.0132	3.10
3	47.76	4.25	14.93	10.17	22.09	1.64 (0.03)	100.84	0.0320	0.0132	3.09
4	45.33	8.12	14.10	9.63	20.82	1.76 (0.01)	99.75	0.0624	0.0145	2.82
5	41.53	15.04	12.79	8.67	18.90	2.07 (0.03)	99.00	0.1187	0.0175	2.33
6	35.66	26.00	10.91	7.39	16.36	2.73 (0.03)	99.05	0.2117	0.0237	1.72
					Fe-loop experiments†					
7	46.91	0.00	14.52	9.81	21.76	7.95 (0.05)	100.96	0.0000	0.0664	1.50
8	45.47	2.17	14.26	9.67	21.16	8.21 (0.07)	100.95	0.0164	0.0690	1.44
9	44.34	3.93	13.88	9.41	20.50	8.57 (0.04)	100.63	0.0299	0.0727	1.37
10	41.73	8.11	12.91	8.81	19.13	9.34 (0.09)	100.02	0.0629	0.0806	1.24
11	37.69	14.45	11.80	7.99	17.36	10.47 (0.12)	99.76	0.1146	0.0924	1.08
12	31.62	25.09	9.66	6.36	14.94	13.26 (0.14)	100.93	0.2034	0.1196	0.83

Note: MeO = metal oxide (NiO or FeO), s.d. = standard deviation.
* Samples were equilibrated in a single run at 1301 °C and $10^{-8.40}$ atm f_{O_2} for 50 hours; (f_{O_2} values were calculated from known CO/CO_2 gas ratios), liquid NiO as a standard state.
† Samples were equilibrated in a single run at 1301 °C and $10^{-12.65}$ atm f_{O_2} for 44 hours, (f_{O_2} calculated), liquid FeO as a standard state (see text for details).

Institut für Mineralogie (J.W. Goethe-Universität, Frankfurt), using a Merchantek LUV213 petrographic ultraviolet Nd-YAG laser microprobe coupled with a Finnigan MAT ELEMENT2 high-resolution ICP double-focusing mass spectrometer. The analytical procedure is similar to that described by Lahaye et al. (1997). The laser was run at a pulse frequency of 10 Hz and pulse energy of 1 mJ for a 60 µm spot size. For a 20 µm crater, the pulse frequency has been increased to 20 Hz, while the pulse energy is decrease down to 0.25 mJ.

The experimental glasses MP12 and MP3 with known Pd contents (INAA, Borisov et al. 1994) were used as external Pd standard. Additionally, synthetic NIST SRM 612 glass has been used as a standard for Pd, Pt, and Rh. The concentrations reported by Sylvester and Eggins (1997) and ^{44}Ca as reference isotope were used for quantification. Five elements were analyzed at low resolution ($\Delta M/M$ = 400). Several isotopes of the same element were chosen in order to evaluate possible interferences. No significant differences were observed between ^{194}Pt and ^{195}Pt. Palladium 108 provides more accurate results possibly because of the Ar-Cu-(H) molecular species interfering on ^{105}Pd and ^{106}Pd. Cadmium also should be monitored because of its interference on ^{108}Pd when using the NIST SRM 612 standard (30 ppm Cd, Pearce et al. 1997).

In some analyses, Pd-containing metal nuggets were encountered (see below in the section "The Pd solubility in silicate melts at reducing conditions and the formation of nuggets"). In such glasses, additional analyses were made in nugget-free areas. In a few cases, the density of nuggets was so high that the analysis of nugget-free areas was impossible. Data on these samples were discarded.

Six glasses with the highest Pd contents (air conditions, DATii-20 series) also were analyzed with the EMP (25 kV, 400 nA, 600 s measurement conditions) to determine the dependence of Pd concentration on TiO_2 independently. The Pd-enriched glass DAT32-20, analyzed with LA ICP-MS, was used as EMP standard to calculate the Pd content in all glasses of the series. The results of EMP measurements are similar to those obtained with the ICP (see Table 1). However, the accuracy of the ICP data is higher. Therefore, ICP measurements are considered to be more reliable.

Results and discussion

All Pd-bearing glasses melted at reducing conditions are black and non-transparent, the glasses prepared in air and CO_2 are transparent, from yellowish to yellow-brown. The Ni-containing glasses are black and non-transparent. The Fe-bearing, TiO_2-free glass is aquamarine. Addition of TiO_2 changes the color of the glass from light brown to completely black.

Accuracy and reproducibility of our Pd data range from very good to reasonable. In one measurement session, where the MP12 glass (61 ppm Pd) was used as an external standard, the Pd content of MP3 was found to be 2.15 ± 0.17 ppm (1σ, an average of 4 measurements), in excellent agreement with 2.2 ppm expected. The Pd content in NIST SRM 612 glass is 1.31 ± 0.26 ppm, which is slightly higher than the tabulated value of 1.09 ± 0.09 ppm (1σ, Sylvester and Eggins 1997). In another measurement session, where the NIST SRM 612 glass was used as an external standard, the Pd content of MP3 was found to be 1.65 ± 0.22 ppm (1σ, an average of 4 measurements), which is 25% lower than the expected concentration (2.2 ppm).

The experimental conditions and the results of Pd, Ni, and Fe solubilities are given in Tables 1 and 2.

The effect of TiO_2 on Pd solubility in silicate melts at oxidizing conditions

In Figure 1, the results of the Pd solubilities at oxidizing conditions are displayed. Two runs were made at fixed T-f_{O_2} conditions and the TiO_2 content in the silicate melts was the only variable (Nos. 1–12 in Table 1). We will first discuss the more reliable data from LA ICP-MS analyses.

There is a clear difference in Pd contents between Ti-poor and Ti-rich melts. Up to approximately 4 wt% TiO_2, the solubility is constant within experimental error at a level of 256 ppm in air and 41.4 ppm in pure CO_2. These solubilities are in reasonable agreement (19 and 26% higher) with 214 ppm and 32.9 ppm Pd obtained from extrapolation of earlier data by Borisov et al. (1994) at similar melt composition.

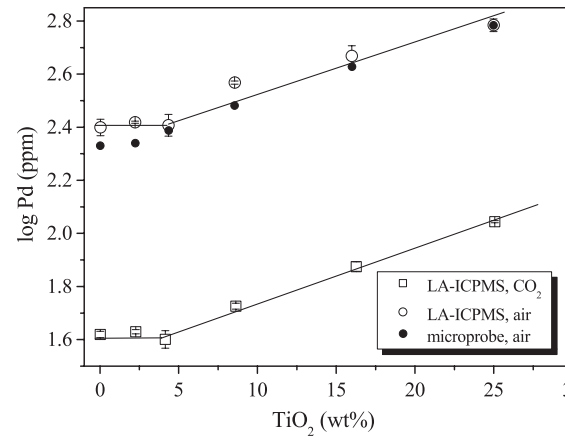

Figure 1. Dependence of Pd solubility on TiO_2 contents in silicate melts at oxidizing conditions and 1300 °C. The solubility in air is about a factor of 6 higher than in CO_2, but the shapes of both curves are identical. Results of microprobe analyses are indicated with full symbols.

At TiO_2 contents above 4 wt%, the Pd solubility increases (Fig. 1). All data from DAT5 to DAT32 (Nos. 3–6, 9–12 in Table 1) were fitted with a single regression yielding the equation (R^2 = 0.995):

$$\log \text{Pd (ppm)} = 0.34 \cdot \log f_{O_2} + 0.019 \cdot \text{TiO}_2 \text{ (wt\%)} + 2.585 \quad (1a)$$

At low TiO_2 contents, there appears to be a plateau in the log Pd vs. TiO_2 relationship in Figure 1, although it cannot be resolved statistically. A regression of all oxidizing data points (Nos. 1–12 in Table 1) gave the same R^2 of 0.995 and very similar coefficients:

$$\log \text{Pd (ppm)} = 0.34 \cdot \log f_{O_2} + 0.017 \cdot \text{TiO}_2 \text{ (wt\%)} + 2.611 \quad (1b)$$

From these equations, it follows that an increase of the TiO_2 content by 16–17 wt% at given oxygen fugacity will increase the Pd solubility by a factor of two.

The slope of 0.34 ± 0.01 for the dependence of the log of Pd solubility vs. the log of the oxygen fugacity is in excellent agreement with a slope of 0.33 ± 0.01 found by Borisov et al. (1994) for the Pd solubility at 1350 °C and at oxidizing conditions. This slope is equivalent to an apparent Pd valence of about +1.33. This unusual valence may result from a mixture of Pd^{1+} and Pd^{2+} present in the melt or, alternatively, reflect the existence of complexes $2Pd^{2+}Pd^0$ dissolved in silicate melts, as discussed by Borisov et al. (1994).

The microprobe data for Pd in the samples produced in air are considered less reliable than the LA ICP-MS data (see previous section), primarily because of the low count rate. Nevertheless, these data also demonstrate constant Pd solubility to about 2.2 wt% TiO_2 and then a strong increase of Pd solubility with increasing TiO_2 (see Fig. 1), which supports the presence of a discontinuity in the log Pd vs. TiO_2 relationship (Fig.1).

The Pd solubility in silicate melts at reducing conditions and the formation of nuggets

The solubility data obtained at low f_{O_2} are less complete with regard to variations in TiO_2 contents. In most cases, we have analyzed only two samples with different TiO_2 concentrations at a given oxygen fugacity. The samples of the DAT3 series were prepared later and, in addition, samples DA and DAT5 were found to be contaminated with micronuggets (see below). As a result, we have a sufficiently large data set on Pd solubility only for Ti-rich melts (Nos. 13–24 in Table 1). All these data were fitted to a single regression and the following equation was obtained ($R^2 = 0.912$):

$$\log \text{Pd (ppm)} = 0.20 \cdot \log f_{O_2} + 0.016 \cdot TiO_2 \text{ (wt\%)} + 1.954 \quad (2)$$

In Figure 2, the experimental data are displayed in a plot of Pd solubility vs. $\log f_{O_2}$ along with the calculated isopleths of Pd solubility in silicate melt with constant TiO_2 contents: 26.7 wt% (average for DAT32 samples), 17.0% (average for DAT17 samples), 9.6% (average for DAT10 samples), and 4.0%. If our results at oxidizing conditions (see Fig. 1) are also valid at reducing conditions, the 4 wt% limit might be a boundary between Ti-rich and Ti-poor melts where the structural position of Pd-oxides in the silicate melt changes.

In spite of some scatter in Figure 2, it is clear that the present data and Equation 2 are in basic agreement with the data of Borisov et al. (1994). The slope of 0.20 ± 0.03 agrees within error limits with the slope of 0.17 ± 0.01 found by Borisov et al. (1994) for Pd solubility at reducing conditions.

As mentioned above, some of our glasses produced under reducing conditions suffer from nugget formation and are thus characterized by high bulk concentrations of Pd (up to 120 ppm). Surprisingly, we found Pt and Rh at the ppm level in all contaminated glasses, although all samples were melted with pure Pd loops. We emphasize that local enrichments of NM discussed below are independent of the true NM solubilities, Pd in nuggets is present as metal, although the stable Pd species dissolved in silicates are Pd-oxides and both behave independently, as shown below.

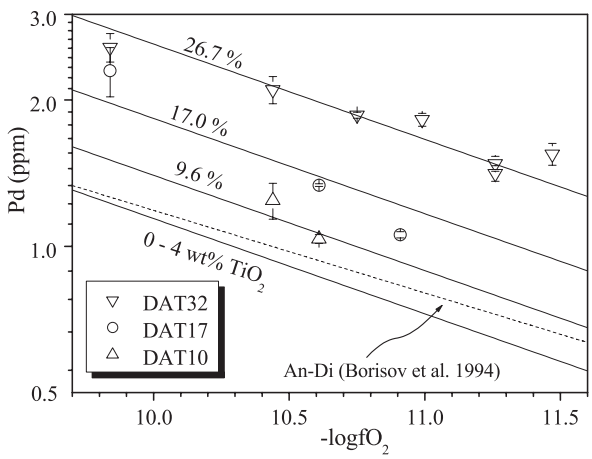

FIGURE 2. Dependence of Pd solubility on TiO_2 contents in silicate melts at reducing conditions. Comparison with earlier data (Borisov et al. 1994, dashed line) and isopleths of Pd solubility in melts with different TiO_2 contents (solid lines) are also shown (see text for details).

The presence of Pd-containing nuggets in this study was surprising because, in earlier experiments, there was no evidence for Pd- or Au-containing nuggets (Borisov et al. 1994; Borisov and Palme 1996), whereas in solubility experiments with Ir, Pt, Rh, or Os (Borisov and Palme 1995, 1997; Ertel et al. 1999; Borisov and Walker 2000) nuggets were encountered frequently.

Analyses of starting materials (DA glass) gave Pd and Rh contents below 0.04 ppm, whereas the starting materials of other samples had Pt contents as high as 6 ppm. This finding is not surprising, as this starting material had been prepared in Pt crucibles (Astrid Holzheid, personal communication). If aliquots of the glasses used in the present experiments contained Pt nuggets, they would act as preferred host phases for precipitation of Pd during experimental runs. This possibility, however, cannot be the only explanation for the formation of Pd nuggets. For example, one of the strongly contaminated glasses, DA-1, which could not be used for the analysis of dissolved Pd contains 225 ppm Pd and only 1.3 and 1.8 ppm Rh and Pt, respectively. This sample was equilibrated with Pd-metal in the same run as sample DAT17-1 (Table 1), which was free of nuggets. Apparently, in this case Rh and Pt are dissolved in Pd nuggets. It is quite possible that the presence of *any* kind of NM nuggets in the starting glass will trigger the growth of all kinds of nuggets or even the formation of new nuggets.

Unfortunately, it seems that even the use of extra-pure starting material cannot guarantee that nuggets will not form. All our contaminated glasses also contained, along with Pt, Rh at a level of 1–3 ppm, which was absent in the starting material. The source of this Rh is probably the furnace. The colder parts of a ceramic sample holder and a tube that have been used for a long period of time are known to be covered with layers of crystalline Pt and probably also Rh. Thus, a silicate sample may be contaminated either mechanically by tiny pieces of Pt or through the vapor phase by Pt/Rh vapors of previously deposited layers of Pt/Rh.

The effect of TiO_2 on Ni and Fe solubilities, NiO and FeO activities in silicate melts

Experiments on Ni and Fe solubilities (Table 2) in melts with variable TiO_2 contents were carried out to determine whether the difference in Pd-solubility between Ti-poor and Ti-rich melts is only related to Pd (or even an artifact), or whether this is a more general phenomenon affecting also other metals. As demonstrated above, the plateau of constant Pd solubility at low TiO_2 is statistically not well defined because of the relatively high scatter of experimental data. In contrast to the PGE, the Ni- and Fe-containing samples do not suffer from the formation of nuggets. Additionally, the experiments were made at relatively high f_{O_2} conditions in order to keep Ni and Fe concentrations in the melt high and statistical errors of the EMP analyses low.

The NiO content in Ti-free, anorthite-diopside eutectic composition (DA) is 1.62 ± 0.03 (1σ) wt% at 1301 °C and $\log f_{O_2} = -8.40$. The calculation of the NiO-solubility using the regression of solubility vs. temperature and f_{O_2} (parameters from Table 2 in Holzheid et al. 1994) gives a slightly lower solubility of 1.21 ± 0.21 wt% (the error is equivalent to an uncertainty in $\log f_{O_2}$ of ±0.1). A possible reason for this discrepancy may be the large

extrapolation in f_{O_2} that is required to compare the Holzheid et al (1994) data with those obtained here. Indeed, with the same melt composition, Borisov and Walker (2000) also found Ni solubility at oxidizing conditions and a temperature of 1400 °C about 30% higher than data extrapolated from Holzheid et al. (1994).

The dependence of Ni solubility on the TiO_2 contents of the silicate melts is given in Table 2. It appears that TiO_2 contents of up to approximately 4 wt% do not affect the solubility. At higher TiO_2 concentrations (up to 26 wt%) the solubility increases from 1.64 wt% NiO to 2.73 wt% NiO. Such a difference in solubility is equivalent to an apparent $\Delta\log f_{O_2}$ of about 0.44, assuming ideal dependence of Ni solubility on oxygen fugacity.

Titanium-rich compositions (Nos. 3–6 in Table 2) were fitted to calculate the dependence of the NiO solubility on TiO_2 contents ($R^2 = 0.998$), and the following equation was obtained:

$$\log \text{NiO (wt\%)} = 0.010 \cdot \text{TiO}_2 \text{ (wt\%)} + 0.165 \quad (3).$$

Extrapolation of Equation 3 to zero TiO_2 leads to a NiO content of 1.46 wt% instead of 1.62 wt% found in the experiment, with the difference exceeding 5σ (see Table 2), obviously beyond statistical error. Thus, in contrast to Pd, the constant Ni solubility at low TiO_2 contents is statistically significant. The different behavior of NiO between low- and high-Ti glasses is clearly seen in Figure 3, where the data are presented in terms of NiO activity coefficients. For comparison with literature data, we used liquid NiO as a standard state for calculating the activity coefficients (Equation 7 in Holzheid et al. 1997). The γ_{NiO} value of 3.1 is practically constant up to 3 mol% TiO_2 and lies within the range (2.70 ± 0.52) suggested by Holzheid et al. (1997) for a broad range of melt compositions. At higher TiO_2 content, there is an excellent correlation ($R^2 = 1.000$) between $\log \gamma_{NiO}$ and X_{TiO_2} (see Fig. 3):

$$\log \gamma_{NiO} = -1.427 \cdot X_{TiO_2} + 0.538 \quad (4)$$

Thus, in rutile-saturated melts, the γ_{NiO} value of 1.7 is roughly two times lower than in TiO_2-free melts, reflecting a corresponding increase in NiO concentrations.

The data on Fe solubility in silicate melts are given in Table 2. At 1301 °C and $\log f_{O_2} = -12.65$, the FeO content in silicate melts increases roughly by 70% from 7.95 wt% in TiO_2-free melt to 13.26 wt% at a TiO_2 content of about 25 wt%. Such a difference in solubility is equivalent to an apparent $\Delta\log f_{O_2}$ of about 0.44. The region of constant solubility at low TiO_2 concentrations, which is characteristic of Ni (and perhaps Pd), is not observed for Fe.

All data (Nos. 7–12 in Table 2) were fitted to obtain the dependence of the Fe solubility on the TiO_2 content ($R^2 = 0.998$):

$$\log \text{FeO (wt\%)} = 0.009 \cdot \text{TiO}_2 \text{ (wt\%)} + 0.897 \quad (5)$$

Apparently, the coefficients for the solubilities of Ni and of Fe as functions of TiO_2 are very similar, 0.0103 ± 0.0003 (1σ) and 0.0089 ± 0.0002 (1σ) for NiO and FeO, correspondingly.

In Figure 3, the data are presented in terms of FeO activity coefficients. Again, we use liquid FeO as a standard state in the calculation of the activity coefficients (Equation 9 in Holzheid et al. 1997). The γ_{FeO} value of 1.50 for the TiO_2-free DA melt lies within the range (1.70 ± 0.52) suggested by Holzheid et al. (1997) for any melt composition. However, increasing the TiO_2 content results in a dramatic decrease of γ_{FeO} ($R^2 = 0.998$):

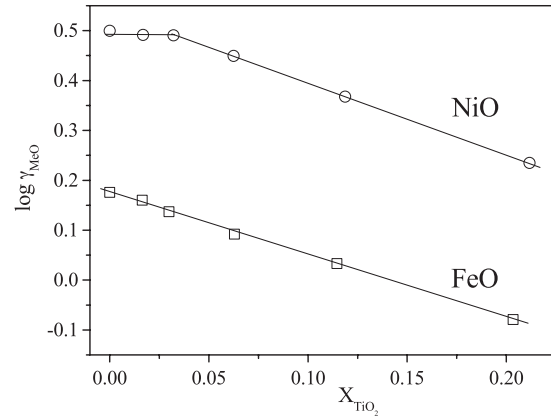

FIGURE 3. Dependence of NiO and FeO activity coefficients on TiO_2 contents in silicate melts. The behavior of NiO is similar to that of Pd (Fig. 1), but at low TiO_2 concentrations different from FeO.

$$\log \gamma_{FeO} = -1.258 \cdot X_{TiO_2} + 0.176 \quad (6)$$

The coefficients of X_{TiO_2} are very similar for $\log \gamma_{FeO}$ (–1.258 ± 0.019, 1σ) and $\log \gamma_{NiO}$ (–1.427 ± 0.010, 1σ), reflecting similar structural changes in FeO- and NiO-containing melts with increasing TiO_2.

Our present results are in excellent agreement with the results of a recent study by O'Neill and Eggins (2002) on solubilities of Ni, Co, Fe, and Mo at 1400 °C. These authors also used anorthite-diopside eutectic compositions as base, with a few different additives, including about 19 wt% TiO_2. The effect is clear: both NiO and FeO activity coefficients decrease significantly in TiO_2-rich melts in comparison with TiO_2-free melts.

Crystalline phases in experimental charges

Because we have worked at 1300 °C with melts having Di-An eutectic composition (eutectic temperature is 1274 °C), most of our charges are crystal free. The DAT32 composition, however, is rutile saturated at experimental temperatures, at least under oxidizing conditions. Also, the DAT32 composition used in melting experiments with Ni-loops at $f_{O_2} = 10^{-8.40}$ atm contains rutile, practically free of Ni.

We found that in melts of DA32 composition and below a "critical f_{O_2}" (about $10^{-11.3}$ atm at 1300 °C, see Table 1), the liquidus phase rutile is replaced by Mg-Ti oxide phase with the value of Ti/Mg (atomic) exceeding two. As the most TiO_2-rich phase in the MgO-TiO_2 binary is karrooite, we suggest that this phase is a pseudobrookite-type, $MgTi_2O_5$-Ti_3O_5 solid solution with a high fraction of Ti^{3+} in the structure. Such solid solutions have been synthesized in Mg-Ti-O system at very low oxygen fugacities (Borowiec and Rosenqvist 1985; Grey et al. 1994). Small pieces of the Mg-Ti oxide crystals were investigated with a transmission electron microscope (TEM). The results indicate that the Mg-Ti phases indeed have the pseudobrookite structure (F. Brenker, personal communication). Details of this study will

be published elsewhere.

Samples with the DAT32 composition melted in Fe-loops at $f_{O_2} = 10^{-12.65}$ atm also contain a crystalline TiO_2-rich phase having atomic Ti/(Mg + Fe) > two. It should be armalcolite, $(Mg,Fe)Ti_2O_5$, which is known to contain a Ti_3O_5 component in solid solution at strongly reducing conditions (Lindsley et al. 1974; Stanin and Taylor 1980; Borowiec and Rosenqvist 1985, etc.).

The partition coefficient for Pd between rutile and silicate melts in the most Pd-enriched DAT32-20 sample (1301 °C, air) was measured with the EMP. A solid/liquid partition coefficient of $D = 0.07 \pm 0.02$ (1σ, average of 3 analyses of 3 different isometric 30×30 μm rutile crystals) was obtained. Capobianco and Drake (1990) measured partitioning of Pd between spinel and silicate melt at 1450 °C in pure oxygen and found the D value to be below 0.02. Capobianco et al. (1994) also found Pd to be mostly incompatible with magnetite and hematite solid solutions crystallizing from silicate melt at 1275 °C and at relatively oxidizing conditions. Recently, Brenan et al. (2003) found Pd to be incompatible with olivine over a wide f_{O_2} range. On the other hand, rutile/melt partitioning of other PGE may be much higher. For example, Hrovat et al. (1996) synthesized rutile with 9.4 mol% RuO_2 at 1300 °C.

The significance of similarities in Pd, Ni and Fe solubilities

As mentioned in the introduction, the systematic study of the NM solubilities in silicate melts is difficult primarily because of experimental problems related to nugget formation. Some investigators believe that the solubilities of NM in natural melts are orders of magnitude higher than the solubilities in synthetic, Fe-free systems (see discussion in Borisov and Palme 2000). The effects of melt composition on the solubilities of Fe-group metals (Ni, Co, Fe) are, however, relatively well understood (e.g., Holzheid et al. 1997; O'Neill and Eggins 2002). Thus, from a comparison of Fe and Ni with Pd, it may be possible to obtain a better understanding of Pd solubility in natural melts.

Although the slope of the correlation of log Ni vs. TiO_2 (Equation 3) is lower than that of the correlation with Pd (Equations 1 and 2), the general behavior of both, Ni and Pd, in Ti-poor and Ti-rich melts is very similar. The behavior of Fe is also not very different from that of Ni and Pd.

As noticed earlier, the stoichiometry of Pd oxides present in the silicate melt is not well understood (see Borisov et al. 1994, for details). On the other hand, the stable species of Ni and Fe in silicate melts are doubtless FeO and NiO (e.g., Holzheid et al. 1994, 1997). Furthermore, the effect of liquid composition on NiO and FeO activity coefficients is relatively small (Doyle 1988; Holzheid et al. 1997; O'Neill and Eggins 2002). The similarities between Ni and Fe with Pd, as described above, suggest that the dependence of the Pd solubility on composition should be similar to that of Fe and Ni. As other NM show a behavior similar to Pd (Borisov and Palme 2000), one may expect that all NM behave in silicate melts qualitatively the same as Fe and Ni. Because Ni and Fe solubilities show little dependence on silicate melt composition, NM solubilities should also be largely independent of melt composition.

The dependence of the NM solubilities on oxygen fugacity dominates over the effects produced by changes in bulk compositions. For example, Borisov and Palme (1997) showed that the difference in Pt solubility between "basaltic" (DA) and "granitic" ($3SiO_2 \cdot MgO \cdot Al_2O_3$, by wt.) melts corresponds to a change of 0.5 log units in f_{O_2}. Therefore, the behavior of NM dissolved as oxides in natural (i.e., "dirty") melts should be very similar to that in "pure" synthetic melts used in the experiments.

However, on the other hand, there is no doubt that melt composition does affect NM solubilities, as shown by the Pt-example or present Pd investigations. The details, however, require further studies. A first-order assumption is that the effects of melt composition on NM solubilities are roughly similar to the effects of melt composition on the solubilities of the Fe-group elements.

A possible reason for the different behavior of Ni and Pd in Ti-poor and Ti-rich liquids

Why does Ni, and probably also Pd, behave so differently in low- and high-Ti melts? One possibility is that the addition of TiO_2 to the melt produces structural changes of the melt at around 4% TiO_2 so that with further addition of TiO_2, more Ni and Pd is accepted. Dickinson and Hess (1985) found relatively constant rutile solubilities in peraluminous melts in the K_2O-Al_2O_3-SiO_2 system but much higher TiO_2 solubilities in peralkaline melts. These results cannot, however, be applied to the melt compositions studied here, as the (Mg + Ca)/Al atomic ratio of about 2.2 is practically constant in all melt compositions used in this study and NBO/T decreases only slightly and very smoothly from about 0.95 in TiO_2-free melts to about 0.66 in TiO_2-saturated melts. Thus it is the change in the TiO_2 content *itself* that produces structural changes in the melt, which then allows more Ni and Pd to be incorporated.

The structural role of Ti in silicate melts is complex and not well understood, although recent studies of natural and synthetic Ti-bearing glasses with extended *K*-edge X-ray absorption fine structure spectroscopy (EXAFS) and high-resolution X-ray absorption near-edge structure spectroscopy (XANES) have provided new insights. Fivefold-coordinated Ti, located in distorted square pyramids, appears to be the dominant Ti species in silicate glasses (e.g., Farges et al. 1996), although four and sixfold coordinated Ti also may be present.

Farges (1997) has studied Ti coordination in glasses of the $Na_2Si_4O_9$-$Na_2Ti_4O_9$ binary and found large changes in Ti coordination depending on total Ti concentration. The $^{VI}Ti/^{V}Ti$ ratio decreases from 5.7 in Ti-poor melt (2 mol% TiO_2) to 1.3 in Ti-rich melts (60 mol% TiO_2, the primary data are taken from Tables 1 and 3 in Farges 1997). A XANES study of natural glasses (Farges and Brown 1997) revealed that in Ti-poor basaltic and trachytic glasses significant fractions of the total Ti (up to 50%) could be in octahedral coordination. On the other hand, although Ti in TiO_2-rich glasses is predominantly five-coordinated, a significant fraction of Ti seems to be located in Ti-rich domains in the glass structure (Farges 1999).

Henderson et al. (2002) also reported changes of Ti coordination in silicate melts with increasing TiO_2 contents. In the TiO_2-Na_2SiO_3 binary, they found that ^{IV}Ti prevails in melts with 1% TiO_2, but at 14% TiO_2, the Ti is present almost exclusively as ^{V}Ti. In TiO_2-$CaSiO_3$ binaries, which may be more appropriate for our DAT compositions, there is a similar effect, although here Ti coordination changes from fivefold in low-Ti melts to

fourfold in high-Ti melts.

Thus, it is conceivable that in the DAT melts used in the present experiments, there is a critical concentration boundary at about 3 mol% TiO_2. At lower TiO_2 concentrations, Ti is present as a species that does not affect Ni and, probably Pd solubilities, at higher TiO_2 contents, Ti produces changes in the melt structure that allow accepting more Ni and Pd-oxides with increasing TiO_2 contents.

The role of TiO_2 in mantle melts

Being a minor component in terrestrial natural liquids, TiO_2 is nevertheless considered a possible candidate for affecting the activities of the various oxide species (SiO_2, FeO, etc.) present in mantle melts. For example, Xirouchakis et al. (2001), following their high-pressure experiments, found a large effect of the TiO_2 content on the activity coefficient of SiO_2 in silicate melts, especially pronounced at TiO_2 contents above 5 mol%. By linear extrapolation of this trend down to the TiO_2 level of primary mantle melts (see Fig. 2 in Xirouchakis et al. 2001), the authors concluded that primary melts would have higher SiO_2 activity coefficients (γ_{SiO_2}) compared with Ti-free melts. This higher γ_{SiO_2} would therefore result in lower SiO_2 contents of primary melts, as the activity of SiO_2 is fixed by the presence of olivine and orthopyroxene.

Our finding of two concentration ranges with different behavior for TiO_2 demonstrates that extrapolation of trends seen at high TiO_2 contents to low TiO_2 contents is not justified in all cases. For example, Xirouchakis et al. (2001) favored a uniform increase of γ_{SiO_2} over the whole range of TiO_2 contents based on their own data and on literature data. However, the results of at least one of their experimental series (1360 °C and 1.2 GPa total pressure) may be interpreted in another way. The values of γ_{SiO_2} obtained in those runs seem to be constant within the error limits (0.58 ± 0.01) at X_{TiO_2} of up to 0.05 (see Table 6 in Xirouchakis et al. 2001), and only with further increases in TiO_2 did these authors note a sharp increase in γ_{SiO_2}, up to 0.73 at $X_{TiO_2} = 0.15$.

By analyzing Mg and Fe olivine/melt partitioning at various TiO_2 contents in the melt, Jones (1988, page 562) suggested that "Ti appears to reduce the FeO activity in silicate melts." Indeed, assuming $(\gamma_{MgO}/\gamma_{FeO})^{Ol}$ as nearly constant and γ_{MgO}^{melt} independent of composition, olivine/melt Fe/Mg K_D should be proportional to γ_{FeO} in the coexisting silicate melt. If so, an increase of 1 mol% of TiO_2 in a primary mantle melt is equivalent to the increase of K_D by about 3%, which is perhaps too small to be relevant. This is obviously not the case for the high-Ti lunar basalts, where 10 mol% of TiO_2 in the liquid will decrease K_D by approximately 25% (from 0.31 to 0.23). Such effects were indeed found in experiments with analogues of lunar rocks (Longhi et al. 1978; Wagner and Grove 1997) and with synthetic, Ti-doped melts (Xirouchakis et al 2001).

ACKNOWLEDGMENTS

The manuscript was considerably improved by comments of D. Xirouchakis, M. Hirschmann, S.-J. Barnes, and M. Toplis. This study was supported by the Deutsche Forschungsgemeinschaft (DFG) and by the Russian Foundation for Basic Research (project 02-05-64192).

REFERENCES CITED

Barnes, S.J., Boyd, R., Kornelliussen, A., Nilssen., L.P., Often, M., Pedersen, R.B., and Robins, B. (1988) The use of mantle normalization and metal ratios in discriminating the effects of partial melting, crystal fractionation and sulphide segregation on platinum group elements, gold, nickel and copper: examples from Norway. In H.M. Prichard, P.J. Potts, J.F.W. Bowles, and S.J. Cribb, Eds., Geo-platinum 87, Elsevier, London. p. 113–143.

Borisov, A. (2001) Loop technique: dynamic of metal/melt equilibration. Mineralogy and Petrology, 71, 87–94.

Borisov, A. and Nactweyh, K. (1998) Ru solubility in silicate melts: experimental results in oxidizing region. Lunar and Planetary Science, XXIX, Abstract No 1320.

Borisov, A. and Palme, H. (1995) Solubility of Ir in silicate melts: New data from experiments with $Ir_{10}Pt_{90}$ alloys. Geochimica et Cosmochimica Acta, 59, 481–485.

Borisov, A and Palme, H. (1996) Experimental determination of the solubility of Au in silicate melts. Mineralogy and Petrology, 56, 297–312.

Borisov, A and Palme, H. (1997) Experimental determination of the solubility of Pt in silicate melts. Geochimica et Cosmochimica Acta, 61, 4349–4357.

Borisov, A. and Palme, H. (2000) Solubility of noble metals in iron-containing silicate melts as derived from experiments in iron-free systems. American Mineralogist, 85, 1665–1673.

Borisov, A. and Walker, R.J. (2000) Os solubility in silicate melts: new efforts and results. American Mineralogist, 85, 912–917.

Borisov, A., Palme, H., and Spettel, B. (1994) Solubility of palladium in silicate melts: implications for core formation in the Earth. Geochimica et Cosmochimica Acta, 58, 705–716.

Borowiec, K. and Rosenqvist, T. (1985) Phase relations and oxygen potentials in Fe-Ti-Mg-O system. Scandinavian Journal of Metallurgy, 14, 33–43.

Brenan, J.M., McDonough, W.F., and Dalpé C. (2003) Experimental constraints on the partitioning of rhenium and some platinum-group elements between olivine and silicate melt. Earth and Planetary Science Letters, 212, 135–150.

Capobianco, C.J. and Drake, M.J. (1990) Partitioning of ruthenium, rhodium, and palladium between spinel and silicate melt and implications for platinum group element fractionation trends. Geochimica et Cosmochimica Acta, 54, 869–874.

Capobianco, C. J., Hervig, R.L., and Drake, M. (1994) Experiments on crystal/liquid partitioning of Ru, Rh, and Pd for magnetite and hematite solid solutions crystallizing from silicate melt. Chemical Geology, 113, 23–43.

Dickinson, J.E. and Hess, P.C. (1985) Rutile solubility and titanium coordination in silicate melts. Geochimica et Cosmochimica Acta, 49, 2289–2296.

Dingwell, D.B. (1992a) Density of some titanium-bearing silicate liquids and the compositional dependence of the partial molar volume of TiO_2. Geochimica and Cosmochimica Acta, 56, 3404–3407.

Dingwell, D.B. (1992b) Shear viscosity of alkali and alkaline earth titanium silicate liquids. American Mineralogist, 77, 270–274.

Doyle, C.D. (1988) Prediction of the activity of FeO in multicomponent magma from known values in [SiO_2-$KAlO_2$-$CaAl_2Si_2O_8$]-FeO liquids. Geochimica et Cosmochimica Acta, 52, 1827–1834.

Doyle, C.D. (1989) Effect of substitution of TiO_2 for SiO_2 on a_{FeO} in magma. Geochimica et Cosmochimica Acta, 53, 2631–2638.

Ertel, W., Dingwell, D.B., and O'Neill, H. St. C. (1996) Solubility of tungsten in a haplobasaltic melt as function of temperature and oxygen fugacity. Geochimica et Cosmochimica Acta, 60**,** 1171–1180.

Ertel, W., O'Neil, H. St. C., Sylvester, P.J., and Dingwell, D.B. (1999) Solubility of Pt and Rh in haplobasaltic silicate melt at 1300 °C. Geochimica et Cosmochimica Acta, 63, 2439–2449.

Farges, F. (1997) Coordination of Ti^{4+} in silicate glasses: A high-resolution XANES spectroscopy study at the Ti *K*-edge. American Mineralogist, 82, 36–43.

——— (1999) A Ti *K*-edge EXAFS study of the medium range environment around Ti in oxide glasses. Journal of Non-crystalline solids, 244, 25–33.

Farges, F. and Brown, G.E. (1997) Coordination chemistry of titanium(IV) in silicate glasses and melts. 4. XANES studies of synthetic and natural volcanic glasses and tektites at ambient temperature and pressure. Geochimica et Cosmochimica Acta, 61, 1863–1870.

Farges, F., Brown, G.E., Navrotsky, A., Gan, H., and Rehr, J.J. (1996) Coordination chemistry of Ti(IV) in silicate glasses and melts. 2. Glasses at ambient temperature and pressure. Geochimica et Cosmochimica Acta, 60, 3039–3053.

Fortenfant, S.S., Günther, D., Dingwell, D.B., and Rubie, D.C. (2003) Temperature dependence of Pt and Rh solubilities in a haplobasaltic melt. Geochimica et Cosmochimica Acta, 67, 123–131.

Grey, I.E., Li, C., and Madsen, I.C. (1994) Phase-equilibria and structural studies on the solid solution $MgTi_2O_5$-Ti_3O_5. Journal of Solid State Chemistry, 113, 62–73.

Gwinn, R. and Hess, P.C. (1989) Iron and titanium solution properties in peraluminous and peralkaline rhyolitic liquids. Contributions to Mineralogy and petrology, 101, 326–338.

Henderson, G.S., Liu, X., and Fleet, M.E. (2002) A Ti L-edge X-ray adsorption study of Ti-silicate glasses. Physics and Chemistry of Minerals, 29, 32–42.

Holzheid, A., Borisov, A., and Palme, H. (1994) The effect of oxygen fugacity and temperature on solubilities of nickel, cobalt and molybdenum in silicate melts. Geochimica et Cosmochimica Acta, 58, 1975–1981.

Holzheid, A., Palme, H., and Chakraborty, S (1997) The activities of NiO, CoO, and FeO in silicate melts. Chemical Geology, 139, 21–38.

Hrovat, M., Holc, J., Samardžija, Z., and Dražič, G. (1996) The extent of solid solubility in the RuO_2-TiO_2 system. Journal of Materials Research, 11, 727–732.

Jones, J.H. (1988) Partitioning of Mg and Fe between olivine and liquids of lunar compositions: The role of composition, pressure and Ti speciation. Lunar and Planetary Science Conference XIX, 561–562.

Lahaye, Y., Lambert, D., and Walters, S. (1997) Ultraviolet laser sampling and high-resolution Inductively coupled plasma mass spectrometry of NIST and BCR-2G glass reference materials. Geostandard Newsletters, 21, 205–214.

Lindsley, D.H., Kesson, S.E., Hartzman, M.J., and Cushman, M.K. (1974) The stability of armalcolite: Experimental studies in the system MgO-Fe-Ti-O. Proceedings of the 5th Lunar Science Conference, 521–534.

Longhi, J., Walker, D., and Hays, J.H. (1978) The distribution of Fe and Mg between olivine and lunar basaltic liquids. Geochimica et Cosmochimica Acta, 42, 1545–1558.

O'Neill, H.St.C. and Eggins, S.M. (2002) The effect of melt composition on trace element partitioning: an experimental investigation of the activity coefficients of FeO, NiO, CoO, MoO_2, and MoO_3 in silicate melts. Chemical Geology, 186, 151–181.

Pearce, N.J.G., Perkins, W.T., Westgate, J.A., Gorton, M.P., Jackson, S.E., Neal, C.R., and Chenery, S.P. (1997) A compilation of new and published major and trace element data for NIST SRM 610 and NIST SRM 612 glass reference materials. Geostandard Newsletters, 21, 115–144.

Stanin, F.T. and Taylor, L.A. (1980) Armalcolite: an oxygen fugacity indicator. Proceedings of the 11th Lunar Science Conference, 117–124.

Sylvester, P.J. and Eggins, S.M. (1997) Analysis of Re, Au, Pd, Pt, and Rh in NIST glass certified reference materials and natural basalt glasses by laser ablation ICP-MS. Geostandard Newsletters, 21, 215–230.

Toplis, M.J. and Carroll, M.R. (1995) An experimental study of the influence of oxygen fugacity on Fe-Ti oxide stability, phase relations, and mineral-melt equilibria in ferro-basaltic systems. Journal of Petrology, 36, 1137–1170.

Wagner, T.P. and Grove, T.L. (1997) Experimental constraints on the origin of lunar high-Ti ultramafic glasses. Geochimica et Cosmochimica Acta, 61, 1315–1327.

Xirouchakis, D., Hirschmann, M.M., and Simpson, J.A. (2001) The effect of titanium on the silica content and on mineral-liquid partitioning of mantle-equilibrated melts. Geochimica et Cosmochimica Acta, 65, 2201–2217.

MANUSCRIPT RECEIVED JANUARY 23, 2003
MANUSCRIPT ACCEPTED NOVEMBER 20, 2003
MANUSCRIPT HANDLED BY MICHAEL TOPLIS